Nrf2-dependent antioxidant response mediated the protective effect of tanshinone IIA on doxorubicin-induced cardiotoxicity

ZHAOHUI GUO[1-4], MIAO YAN[1,3], LEI CHEN[1,3], PINGFEI FANG[1,3], ZHIHUA LI[1,3,4], ZIMENG WAN[1,3,4], SISI CAO[1,3,4], ZHENYAN HOU[1,3,4], SHANSHAN WEI[1,3], WENQUN LI[1,3] and BIKUI ZHANG[1,3,4]

[1]Department of Pharmacy, The Second Xiangya Hospital, Central South University, Changsha, Hunan 410011; [2]Department of Pharmacy, Wuhan Fourth Hospital (Puai Hospital), Tongji Medical College, Huazhong University of Science and Technology, Wuhan, Hubei 430033; [3]Institute of Clinical Pharmacy, Central South University, Changsha, Hunan 410011; [4]School of Pharmaceutical Sciences, Central South University, Changsha, Hunan 410013, P.R. China

Abstract. Doxorubicin (DOX), a potent and widely used anti-cancer agent, can give rise to severe cardiotoxicity that limits its clinical use by inducing oxidative stress. Nuclear factor (erythroid-derived 2)-like 2 (Nrf2) is the central regulator of cellular responses to electrophilic/oxidative stress, which serves a critical role in maintenance of normal cardiac function. Tanshinone IIA (Tan IIA) has previously been reported to protect against DOX-induced cardiotoxicity. The aim of the present study was to elucidate whether Nrf2 signaling serves a role in the underlying mechanism. In the animal model, DOX induced acute cardiotoxicity, whereas Tan IIA pretreatment reduced the activity of myocardial enzymes, and increased activity of the antioxidant enzymes superoxide dismutase, catalase and glutathione (GSH). Furthermore, Tan IIA pretreatment (3-10 μM) significantly increased the cell viability and markedly restored morphological changes in DOX-injured H9c2 cells, decreased the generation of reactive oxygen species, and increased the level of intracellular GSH. Additionally, Tan IIA pretreatment also induced the nuclear accumulation of Nrf2 and its downstream genes heme oxygenase-1, NAD(P)H dehydrogenase (quinone) 1, and glutamate-cysteine ligase catalytic subunit in both the mice cardiac tissues and H9c2 cells. Nrf2 knockdown by small interfering RNA downregulated Tan IIA-induced Nrf2 activation and reversed the effect of Tan IIA on the DOX-induced inhibition of cell viability. These results suggest that the Nrf2-dependent antioxidant response mediates the protective effect of Tan IIA on DOX-induced cardiotoxicity.

Introduction

Doxorubicin (DOX, also known as adriamycin), a typical anthracycline, ranks as one of the most potent antitumor agents available for breast cancer, lymphoma, and hematologic malignancy (1). Unfortunately, the clinical use of DOX is limited due to the life-threatening cardiotoxicity, which may ultimately develop into cardiomyopathy and congestive heart failure (2). Dose limitation strategy is now most commonly used to reduce the DOX-induced cardiotoxicity, as an association between the quantity of DOX accumulated in the heart and the incidence of cardiac events has been identified (3). However, lower concentrations may preclude successful completion of chemotherapy, causing a dilemma for oncologists and cardiologists (4). Advances in the molecular basis of anthracycline-induced cardiotoxicity indicate that multiple mechanisms are involved, among which reactive oxygen species (ROS) and oxidative stress are the most important factors (5). Furthermore, endogenous antioxidants decreased following the DOX treatment. The administration of antioxidants has been demonstrated to prevent cardiac injury induced by DOX both *in vitro* and *in vivo* (6,7).

Nuclear factor (erythroid-derived 2)-like 2 (Nrf2), a redox-sensitive transcription factor, is the central regulator of cellular responses to electrophilic/oxidative stress. It has previously been revealed that Nrf2 was essential for detoxification gene activity in mammalian cardiac cells (8). Under physiological conditions, Kelch-like ECH-associated protein 1 (Keap1), the cytosolic regulatory protein, was tightly bound to Nrf2 to retain it in the cytoplasm. Nrf2 was then released from Keap1 and translocated to the nucleus in response to oxidants and electrophiles, which may result in the subsequent binding to antioxidant responsive DNA elements (AREs) and activate the transcription of downstream genes, including antioxidants and phase II and phase III detoxification enzymes (9). As DOX-induced oxidative stress is the major cause of injury in cardiac cells (4), enhancing the critical biological functions of Nrf2 should be a safe and effective strategy to counter DOX

Correspondence to: Professor Bikui Zhang or Dr Wenqun Li, Department of Pharmacy, The Second Xiangya Hospital, Central South University, 139 Renmin Road, Changsha, Hunan 410011, P.R. China
E-mail: 505995@csu.edu.cn
E-mail: liwq1204@csu.edu.cn

cardiotoxicity. On this basis, the mechanisms of drug candidates against DOX-induced cardiotoxicity focus on Nrf2, especially the bioactive natural products. For instance, aringenin-7-O-glucoside, a flavonoid isolated from *Dracocephalum rupestre* Hance, protected against DOX-induced cardiomyocyte apoptosis via the nuclear translocation of Nrf2 (10). Similar results were also observed in sulforaphane, a natural isothiocyanate compound in cruciferous vegetables (7). Furthermore, Nrf2 mediated the protective effect of a-Linolenic acid on DOX-induced cardiotoxicity in rats (11).

Tanshinone IIA (Tan IIA), one of the major components isolated from Radix *Salvia miltiorrhiza*, exhibits potent antioxidant activity (12). Emerging experimental studies and clinical trials have demonstrated that Tan IIA prevents oxidative stress-triggered atherogenesis as well as cardiac injury and hypertrophy (13). The protective effect of Tan IIA on DOX-induced cardiotoxicity has been preliminarily investigated (14), but the mechanism remains unknown. In view of the critical role Nrf2 has in DOX-induced cardiotoxicity, the present study aimed to determine whether the Nrf2-dependent antioxidant response mediated the protective effect of Tan IIA on DOX-induced cardiotoxicity *in vivo* and *in vitro*.

Materials and methods

Chemicals and reagents. Sodium Tan IIA sulfonate injection was purchased from Shanghai First Biochemical & Pharmaceutical Co., Ltd. (Shanghai, China); DOX hydrochloride was purchased from Shenzhen Main Luck Pharmaceuticals, Inc. (Shenzhen, China). The detection kit for aspartate aminotransferase (AST) was purchased from Abbott Laboratories Trading Shanghai Co., Ltd. (Shanghai, China). The kit for measuring lactate dehydrogenase (LDH) was purchased from Ningbo Meikang Biotechnology Co., Ltd. (Ningbo, China). The kit for measuring creatine kinase (CK) and creatine kinase-muscle/brain (CK-MB) from Beijing Strong Biotechnologies, Inc. (Beijing, China). Malondialdehyde (MDA; cat. no. A003-1), reduced glutathione (GSH; cat. no. A006-2), superoxide dismutase (SOD; cat. no. A001-3) and catalase (CAT; cat. no. A007-2) assay kits were from Nanjing Jiancheng Bioengineering Institute (Nanjing, China). Dichloro-dihydro-fluorescein diacetate (DCFH-DA) was purchased from Sigma-Aldrich (Merck KGaA, Darmstadt, Germany; cat. no. D6883).

Tan IIA (purity, >98%) was purchased from National Institutes for Food and Drug Control (Beijing, China). DOX, tertbutyl hydroquinone (tBHQ), dimethyl sulfoxide (DMSO) and MTT were purchased from Sigma-Aldrich; Merck KGaA. ROS Assay kit (cat. no. S0033) and BCA protein assay kit (cat. no. P0009) was purchased from Beyotime Institute of Biotechnology (Shanghai, China). Small interfering (si)RNA was purchased from Ribobio Co., Ltd. (Guangzhou, China). Lipofectamine 2000 was purchased from Invitrogen (Thermo Fisher Scientific, Inc., Waltham, MA, USA). Anti-Nrf2 antibody were purchased from Santa Cruz Biotechnology, Inc. (cat. no. sc-722; Dallas, TX, USA). Anti-proliferating cell nuclear antigen (PCNA; cat. no. ab18197) and β-actin (cat. no. ab8226) were purchased from Abcam (Cambridge, UK).

Animals and pharmacological treatments. A total of 30 male Institute of Cancer Research mice weighing 25-29 g

and aged 6 weeks were purchased from Beijing Vital River Laboratory Animal Technology Co., Ltd. (Beijing, China). The mice were given rodent chow 5001 (Beijing Vital River Laboratory Animal Technology Co., Ltd.) and distilled water ad libitum, and housed at room temperature ($24\pm2°C$) under a humidity-controlled ($65\pm5\%$) condition on a regular 12-h light/dark cycle. The mice were randomly assigned to 5 groups (n=6 in each group) as follows: The control (normal saline) group, the DOX (18 mg/kg) group, the Tan IIA (15 mg/kg) + DOX (18 mg/kg) group, the Tan IIA (30 mg/kg) + DOX (18 mg/kg) group, and the Tan IIA (30 mg/kg) group. The dose of Tan IIA (15 and 30 mg/kg) was selected based on the results of a previous study (15). The mice were treated with Tan IIA or 0.2 ml normal saline from day 1 to day 7, and DOX was administered at day 5, the mice were then sacrificed at day 8; all treatments were administered by intraperitoneal injection. The mice in the control (normal saline) group did not receive DOX. All animal use procedures were conducted according to the Regulations of Experimental Animal Administration issued by the State Committee of Science and Technology of the People's Republic of China, with the approval of the Ethics Committee in The Experimental Animal Center of the Second Xiangya Hospital (Changsha, China).

Heart histopathological examination. The mice hearts of each group were harvested immediately following blood collection. Sections of the freshly heart samples were used to analyze biochemical index. The rest of samples were fixed with 4% paraformaldehyde for 24 h at 25°C, and embedded in paraffin blocks. They were then sectioned 4-μm-thick sections and stained with hematoxylin and eosin (HE) at room temperature for 3 min. The structure was examined with a light microscope (magnification, x100) (CKX41; Olympus Corporation, Tokyo, Japan).

Measurement of serum myocardial enzymes. Blood were collected from the heart of anesthetized mouse and centrifuged (1,006.2 x g, 10 min, 4°C) to obtain the serum samples, which were assayed for the determination of serum myocardial enzymes (AST, LDH, CK and CK-MB) using kits with an automatic biochemical analyzer (Abbott Pharmaceutical Co., Ltd., Lake Bluff, IL, USA). The experiments were performed according to the manufacturers' instructions.

Measurement of GSH, SOD, CAT and MDA. The mice hearts were harvested immediately following blood collection. The partial myocardial tissues from each heart was minced and homogenized to prepare for GSH, SOD, CAT, and MDA detection with corresponding kits. The experiments were performed according to the manufacturers' protocol.

Cell culture and treatment. The H9c2 rat myoblast cell line obtained from Xiangya Cell Bank (Central South University, Changsha, China) was cultured in Dulbecco's modified Eagle's medium (Gibco; Thermo Fisher Scientific, Inc., Waltham, MA, USA) supplemented with 10% FBS (Biological Industries, Kibbutz Beit Haemek, Israel) and antibiotics (100 μg/ml streptomycin and 100 U/ml penicillin; Hyclone; GE Healthcare Life Sciences, Logan, UT, USA) in a humidified atmosphere with 5% CO_2 at 37°C.

Table I. Mice primers for quantitative polymerase chain reaction.

Gene	Forward	Reverse
Nrf2	5'-TAGTGCCCCTGGAAGTGTCA-3'	5'-TTGGGATTCACGCATAGGAG-3'
HO-1	5'-AGCCCCACCAAGTTCAAACA-3'	5'-TGCCAACAGGAAGCTGAGAG-3'
NQO1	5'-CAGCCAATCAGCGTTCGGTA-3'	5'-CTTCATGGCGTAGTTGAATGATGTC-3'
GCLC	5'-CAGTCAAGGACCGGCACAAG-3'	5'-CAAGAACATCGCCTCCATTCAG-3'
MRP2	5'-CGCGTCCGGCAGTATATGA-3'	5'-ATAATCTTTGACTCAGTGTGGA-3'
P-gp	5'-CCCATCATTGCAATAGCAGG-3'	5'-GTTCAAACTTCTGCTCCTGA-3'
β-actin	5'-CATCCTGCGTCTGGACCTGG-3'	5'-TAATGTCACGCACGATTTCC-3'

Nrf2, nuclear factor (erythroid-derived 2)-like 2; HO-1, heme oxygenase-1; NQO1, NAD(P)H dehydrogenase (quinone) 1; GCLC, glutamate-cysteine ligase catalytic subunit; MRP2, multidrug resistance-associated protein 2; P-gp, P-glycoprotein.

The cells were incubated with 1 μmol/l DOX for 24 h with or without Tan IIA pretreatment for 4 h at 37°C, except where indicated otherwise. Tan IIA was dissolved in DMSO and diluted with cell culture media to achieve the final concentration (1, 3, 5 and 10 μM). The final concentration of Tan IIA was determined according to previous reported study (16). tBHQ (50 nM), a classical activator of Nrf2, was used to pretreatment cells for 4 h and then treat with 1 μmol/DOX for 24 h.

siRNA transient transfection. The Nrf2 siRNA (sense: 5'-CGU GAAUCCCAAUGUGAAATT-3', antisense: 5'-UGUUUCACA UUGGGAUUCACGTT-3') and negative control siRNA (sense: 5'-CUUCCUCUCUUUCUCUCCCUUGUGA-3', antisense: 5'-UCACAAGGGAGAGAAAGAGAGGAAGGA-3') were synthesized and purchased from Ribobio Co., Ltd. (Guangzhou, China). H9c2 cells were grown in 96-well plates and transiently transfected with 0.5 μg Nrf2 or negative control siRNA constructs using Lipofectamine 2000 transfection reagent, according to the manufacturer's protocol. After incubating at 33°C and 5% CO_2 for 36 h, cells were further treated with DOX and/or Tan II A prior to the MTT and western blot analyses.

Cell viability analysis. Cell viability was determined by MTT assay according to the manufacturer's protocol; DMSO was used to dissolve purple formazan. Percent viability was defined as the relative absorbance of the treated vs. control cells at the wavelength of 490 nm. The morphological changes were detected with a light microscope (magnification, x200).

Measurement of intracellular ROS and GSH. Intracellular accumulation of ROS was determined by measuring the oxidative conversion of cell permeable DCFH-DA to fluorescent dichlorofluorescein (DCF) in a fluorospectrophotometer (model F4000; Hitachi, Ltd., Tokyo, Japan). A total of $2x10^4$ cells were incubated with 0.1 ml DCFH-DA (10 μM) at 37°C for 20 min. DCF fluorescence distribution was detected by fluorospectrophotometer analysis at an excitation wavelength of 488 nm and at an emission wavelength of 535 nm. Intracellular accumulation of GSH was measured using the aforementioned assay kit according to the corresponding manufacturer's protocol.

Reverse transcription-quantitative polymerase chain reaction (RT-qPCR). Total mRNA was extracted from the heart tissue or cells with TRIzol (Life Technologies; Thermo Fisher Scientific, Inc.) and equal amounts of RNA were reverse-transcribed to cDNA using a PrimeScript RT reagent kit with gDNA Eraser (Perfect Real Time; Takara Bio, Inc., Otsu, Japan). cDNA amplification was performed with an initial step for 15 sec at 95°C, followed by 40 cycles (15 sec at 95°C, then 31 sec at 60°C). Data analysis was performed using the 7900HT Sequence Detection System (Applied Biosystems; Thermo Fisher Scientific, Inc.) and the $2^{-\Delta\Delta Cq}$ method (17). The level of β-actin mRNA was used as the internal standard. The primers for real-time PCR analysis are presented in Tables I and II.

Western blotting. The heart tissue of the mice and the cell extracts were prepared in radioimmunoprecipitation assay buffer (Beyotime Institute of Biotechnology). The nuclear and cytoplasmic extracts were harvested with NE-PER nuclear and cytoplasmic extraction reagents (Pierce; Thermo Fisher Scientific, Inc.) using the manufacturer's protocols. The total mass of protein was determined using a BCA assay. Western blotting was performed with some modifications as described (15). Total protein (20 μg/lane) was loaded and separated by 10% SDS-PAGE electrophoresis and transferred to polyvinylidene difluoride membranes. Following blocking in 5% non-fat milk in 0.05% Tween-20/Tris-buffered saline for 1 h at room temperature, the membranes were incubated overnight at 4°C with the following primary antibodies: Nrf2 (1:1,000), PCNA and β-actin (both 1:2,000). The immunoblots were then incubated with horseradish peroxidase-conjugated immunoglobulin G secondary antibodies (goat anti-mouse, cat. no. sc-2005 and goat anti-rabbit, cat. no. sc-2004; both 1:5,000; Santa Cruz Biotechnology, Inc.) at room temperature for 1 h. The membranes were developed with Pierce™ ECL Western Blotting Substrate (cat. no. 32106; Thermo Fisher Scientific, Inc.) according to the manufacturer's protocol. The densities of the bands were determined by an imaging densitometer and the grayscale value of the bands were quantified by ImageJ analysis software (version 1.43; National Institutes of Health, Bethesda, MD, USA). PCNA was used as the nuclear loading control and β-actin was used as the cytosolic loading control.

Statistical analysis. All data were presented as the mean ± standard error of the mean. Statistical analysis

Table II. Rat primers for quantitative polymerase chain reaction.

Gene	Forward	Reverse
Nrf2	5'-CCATGCCTTCTTCCACGAA-3'	5'-AGGGCCCATGGATTTCAGTT-3'
HO-1	5'-GCGAAACAAGCAGAACCCA-3'	5'-GCTCAGGATGAGTACCTCCCA-3'
NQO1	5'-AACGTCATTCTCTGGCCAATTC-3'	5'-GCCAATGCTGTACACCAGTTGA-3'
GCLC	5'-GTCTTCAGGTGACATTCCAAGC-3'	5'-TGTTCTTCAGGGGCTCCAGTC-3'
MRP2	5'-GCTGGTTGGAAACTTGGTCG-3'	5'-CAACTGCCACAATGTTGGTC-3'
P-gp	5'-ATCAACTCGCAAAAGCATCC-3'	5'-AATTCAACTTCAGGATCCGC-3'
β-actin	5'-TACAACCTCCTTGCAGCTCC-3'	5'-GGATCTTCATGAGGTAGTCAGTC-3'

Nrf2, nuclear factor (erythroid-derived 2)-like 2; HO-1, heme oxygenase-1; NQO1, NAD(P)H dehydrogenase (quinone) 1; GCLC, glutamate-cysteine ligase catalytic subunit; MRP2, multidrug resistance-associated protein 2; P-gp, P-glycoprotein.
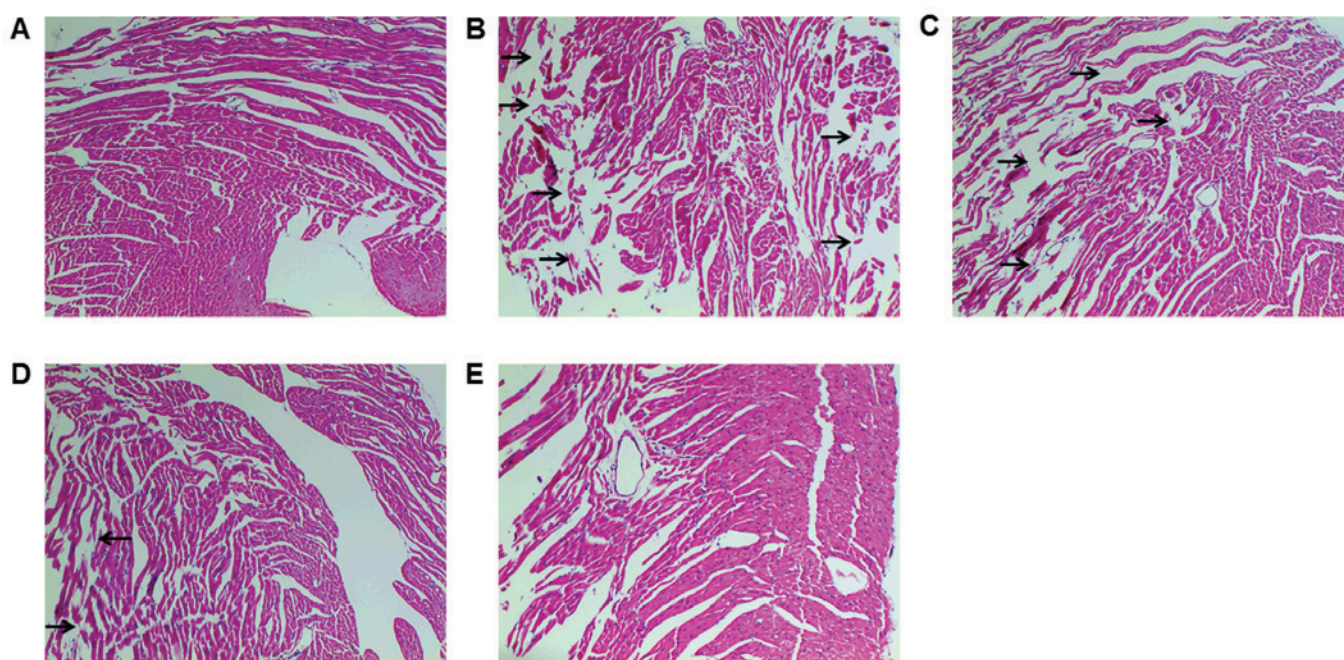

Figure 1. Effect of Tan IIA on DOX-induced pathomorphological changes in mice. Mice were treated with Tan IIA or normal saline from days 1-7 and DOX was administered at day 5. Mice were then sacrificed at day 8 and heart tissues were stained with hematoxylin and eosin. (A) Control; (B) DOX (18 mg/kg); (C) DOX (18 mg/kg) + Tan IIA (15 mg/kg); (D) DOX (18 mg/kg) + Tan IIA (30 mg/kg); (E) Tan IIA (30 mg/kg). Regions of myocardial fiber fragmentation and gap enlargement are indicated by black arrows. The magnification of images is x100. Tan IIA, tanshinone IIA; DOX, doxorubicin.

was performed by analysis of variance followed by the Newman-Student-Keuls test for multiple comparisons using SPSS 19.0 (IBM Corp., Armonk, NY, USA). P<0.05 was considered to indicate a statistically significant difference.

Results

Tan IIA protects against DOX-induced myocardial injury in mice. HE staining was conducted to detect histopathological changes, which demonstrated myocardial fiber fragmentation and gap enlargement in DOX group, which was attenuated by Tan IIA pretreatment (Fig. 1). Serum myocardial enzymes (AST, LDH, CK and CK-MB) are the important indexes that reflect the extent of myocardial injury (18). As presented in Table III, DOX significantly increased the activity of all enzymes compared with controls, indicating cardiotoxicity.

Conversely, Tan IIA significantly inhibited the activity of AST, LDH and CK induced by DOX at 30 mg/kg, and decreased the CK-MB activity at 15 and 30 mg/kg. These findings suggest that Tan IIA can protect against DOX-induced myocardial injury, in accordance with previous studies (13,14).

Antioxidant activity of Tan IIA is associated with its protective effect against DOX-induced cardiotoxicity in mice. The level of SOD, CAT, GSH and MDA were measured to evaluate oxidative stress degree. DOX induced oxidative stress, as indicated by significantly decreased SOD and CAT activities, GSH content and increased MDA production compared with controls. Tan IIA dose-dependently and significantly inhibited the effect of DOX on SOD, CAT, GSH and MDA level in DOX+Tan IIA groups, and thus exhibited potent antioxidant capacity (Table IV).

Table III. Effect of Tan IIA pretreatment on the serum myocardial enzymes.

Group	AST (U/l)	LDH (U/l)	CK (U/l)	CK-MB (U/l)
Control	127.6±14.3	698.7±60.0	1,866.3±279.4	390.3±71.4
DOX (18 mg/kg)	372.3±61.6[a]	1,557.4±214.2[a]	3,002.0±614.1[a]	774.5±205.7[a]
D+T (15 mg/kg)	333.4±110.9	1,249.5±518.8	2,159.7±749.7	471.0±171.0[b]
D+T (30 mg/kg)	183.0±53.2[c]	1,067.3±273.8[b]	1,676.9±767.3[b]	366.4±166.6[c]
Tan IIA (30 mg/kg)	111.9±40.5	570.1±208.4	1,566.5±571.3	336.8±89.6

Data are presented as the mean + standard error of the mean (n=6). [a]P<0.001 vs. control; [b]P<0.01 and [c]P<0.001 vs. DOX. Tan IIA, tanshinone IIA; AST, aspartate aminotransferase; LDH, lactate dehydrogenase; CK, creatine kinase; CK-MB, creatine kinase-muscle/brain; DOX, doxorubicin; D+T, doxorubicin and tanshinone IIA.

Table IV. Effect of Tan IIA pretreatment on antioxidant capacity in mice heart.

Group	GSH (μmol/g)	SOD (U/mg)	CAT (U/mg)	MDA (nmol/mg)
Control	20.2±1.6	106.8±6.1	66.8±5.7	9.5±1.2
DOX (18 mg/kg)	15.0±1.6[b]	79.0±16.8[a]	52.0±4.3[a]	14.4±1.7[b]
D+T (15 mg/kg)	20.5±3.2[d]	107.5±14.3[d]	63.1±5.6[c]	11.2±2.7
D+T (30 mg/kg)	23.5±3.8[e]	118.6±12.3[d]	71.0±9.6[e]	9.2±2.0[d]
Tan IIA (30 mg/kg)	21.4±2.6	108.8±12.7	68.5±8.3	9.0±4.4

Data are presented as the mean + standard error of the mean (n=6). [a]P<0.01 and [b]P<0.001 vs. control; [c]P<0.05, [d]P<0.01 and [e]P<0.001 vs. DOX. Tan IIA, tanshinone IIA; GSH, glutathione; SOD, superoxide dismutase; CAT, catalase; MDA, malondialdehyde; DOX, doxorubicin; D+T, doxorubicin and tanshinone IIA.

Nrf2 signaling is associated with the protective effect of Tan IIA on DOX-induced cardiotoxicity in mice. To determine whether Tan IIA protected against DOX-induced cardiotoxicity via induction of Nrf2 signaling, the expression of Nrf2 and its downstream genes were measured by western blotting and RT-qPCR. The mRNA results demonstrated that, compared with controls, DOX alone had no significant influence on Nrf2, heme oxygenase (HO)-1 and glutamate-cysteine ligase catalytic subunit (GCLC), but significantly raised the mRNA expression of NAD(P)H dehydrogenase (quinone) 1 (NQO1), multidrug resistance-associated protein 2 (MRP2) and P-glycoprotein (P-gp). Compared with DOX alone, Tan IIA pretreatment significantly increased Nrf2, HO-1, NQO1 and GCLC in DOX+Tan IIA groups, but reduced the expression of MRP2 and P-gp (Fig. 2). As presented in Fig. 3A and B, the protein expression of total Nrf2 was significantly increased in the DOX + Tan IIA groups in a dose-dependent manner compared with DOX alone, and Tan IIA alone also induced a significant increase in Nrf2 expression in the heart tissue compared with controls. As nuclear translocation of Nrf2 was the key to activating Nrf2-related pathway, nuclear accumulation and cytoplasmic Nrf2 expression were evaluated. Nuclear Nrf2 expression was similar to total Nrf2, whereas cytoplasmic Nrf2 was decreased in the Tan IIA+DOX group and Tan IIA alone group compared with the DOX or control group (Fig. 3C-E).

Tan IIA protects against DOX-induced injury and oxidative stress in H9c2 cells. In vitro experiments were performed in H9c2 cells. The effect of DOX or Tan IIA treatment alone for 24 h on the viability of H9c2 cells was investigated (Fig. 4A and B). DOX decreased the cell viability in a dose-dependent manner (0.1-1 μM). DOX (1 μM) was used in the subsequent experiments, which was consistent with previous studies (5,11). Tan IIA (1-10 μM) treatment alone exhibited no significant effect on cell viability, but the cell viability was inhibited by Tan IIA at the concentration of 15 and 20 μM. Furthermore, Tan IIA (1-10 μM) pretreatment dose-dependently reversed the inhibitive effect of DOX on cell viability (Fig. 4C). Additional experiments indicated that DOX induced cell rounding and detachment, whereas Tan IIA pretreatment protected the cells from such morphological changes (Fig. 4D).

To determine whether Tan IIA inhibited the DOX-induced generation of ROS in H9c2 cells, the generation of ROS in DOX-treated and Tan IIA + DOX-treated cells were measured via fluorescence microscopy with DCFH-DA as a probe following 24 h incubation (Fig. 4E), in which tBHQ, a classical activator of Nrf2, was used as the positive control. DOX significantly increased the ROS accumulation compared with controls, and co-treatment with Tan IIA dose-dependently ameliorated the ROS levels. As presented in Fig. 4F, DOX treatment resulted in significant decreases of GSH levels, and this inhibition was attenuated by Tan IIA pretreatment, which enhanced the GSH content dose-dependently. These findings suggest that Tan IIA alleviated the DOX-induced oxidative stress.
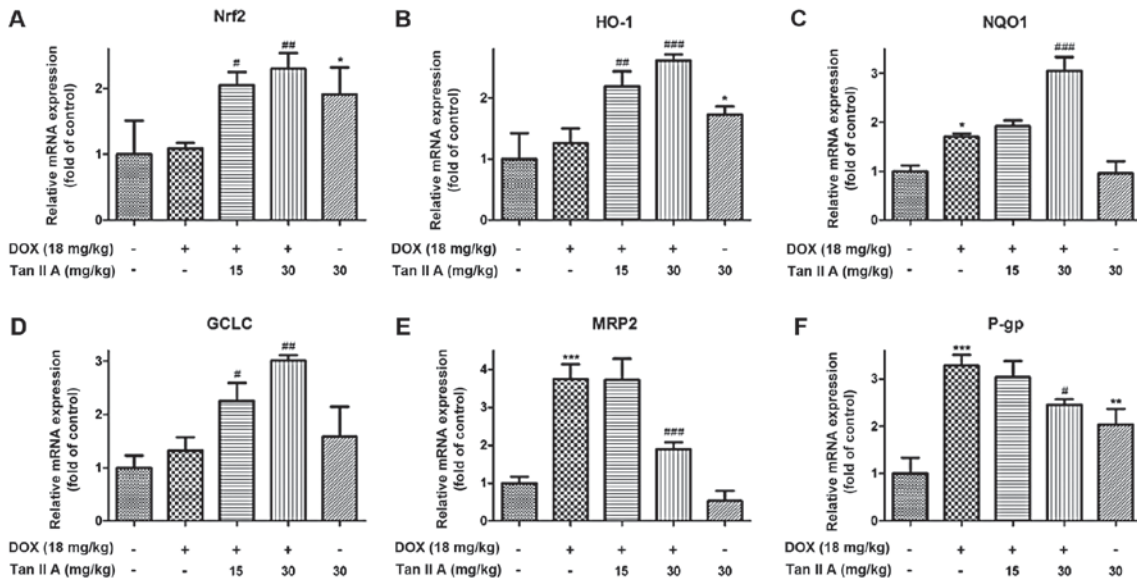
Figure 2. Effect of Tan IIA on Nrf2 mRNA and its downstream genes expression in DOX-treated mice heart. The mRNA expression of (A) Nrf2, and its downstream genes, including (B) HO-1, (C) NQO1, (D) GCLC, (E) MRP2 and (F) P-gp were determined by reverse transcription-quantitative polymerase chain reaction. Data are presented as the mean ± standard error of the mean (n=6). *P<0.05, **P<0.01 and ***P<0.001 vs. the control; #P<0.05, ##P<0.01 and ###P<0.001 vs. DOX. Tan IIA, tanshinone IIA; Nrf2, nuclear factor (erythroid-derived 2)-like 2; DOX, doxorubicin; HO-1, heme oxygenase-1; NQO1, NAD(P)H dehydrogenase (quinone) 1; GCLC, glutamate-cysteine ligase catalytic subunit; MRP2, multidrug resistance-associated protein 2; P-gp, P-glycoprotein.
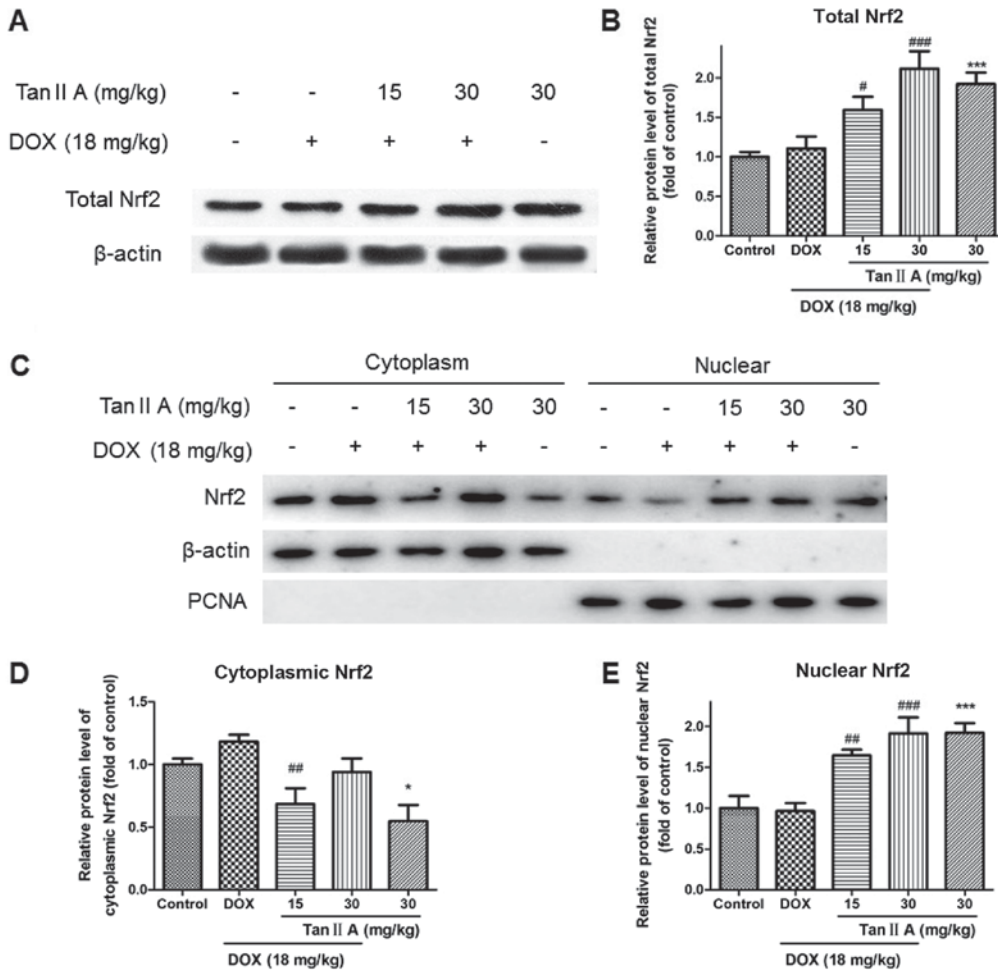

Figure 3. Effect of Tan IIA on Nrf2 protein expression in DOX-treated mice heart. (A) Representative western blotting and (B) quantitative analysis of total Nrf2 protein expression. (C) Representative western blotting and (D and E) quantitative analysis of nuclear and cytoplasmic Nrf2 protein expression. Data are presented as the mean ± standard error of the mean (n=6). *P<0.05 and ***P<0.001 vs. the control; #P<0.05, ##P<0.01 and ###P<0.001 vs. DOX. Tan IIA, tanshinone IIA; Nrf2, nuclear factor (erythroid-derived 2)-like 2; DOX, doxorubicin; PCNA, proliferating cell nuclear antigen.
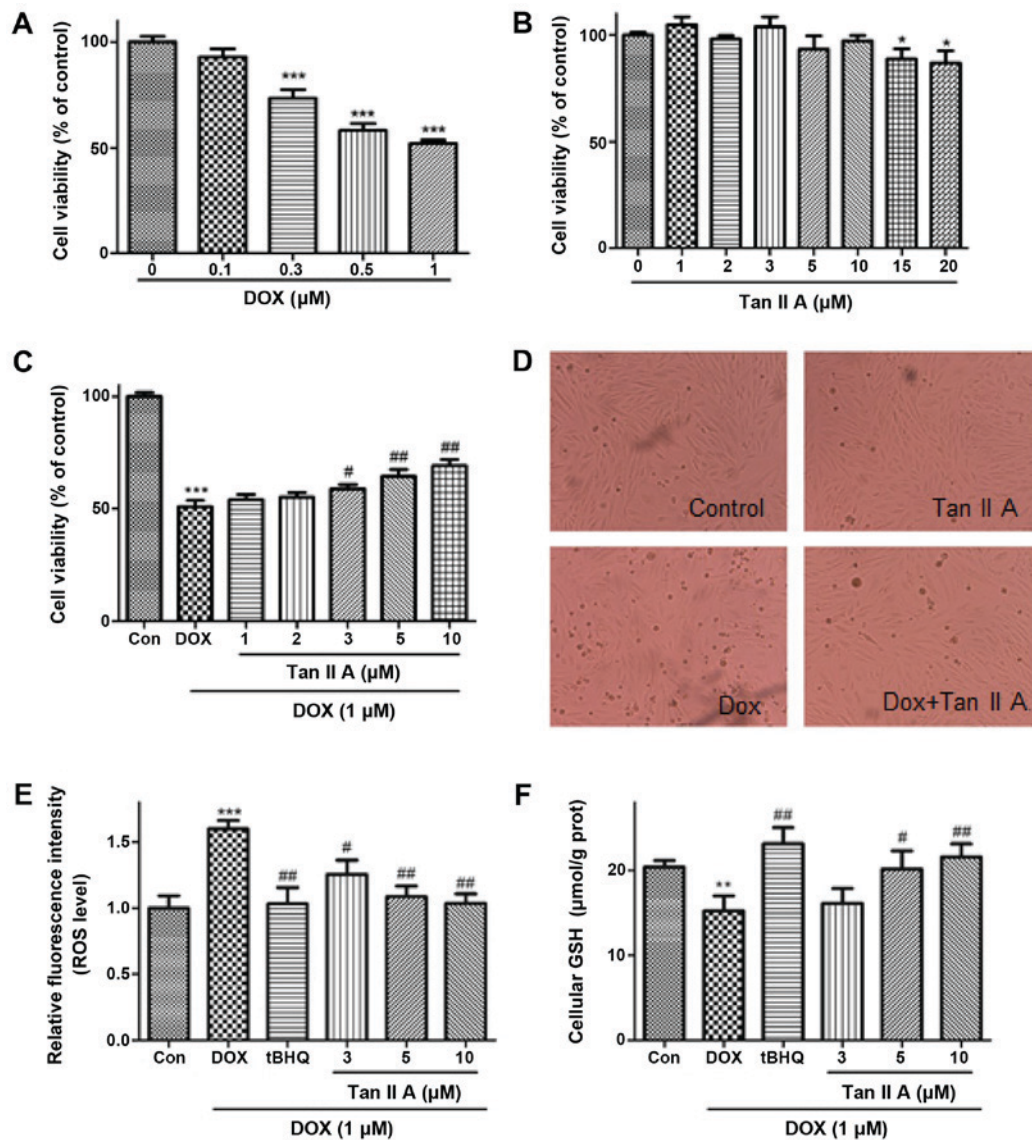
Figure 4. Effect of Tan IIA on DOX-induced cell injury and oxidative stress in H9c2 cells. Cells were incubated with increasing concentrations of (A) DOX (0-1 μM) for 24 h or (B) Tan IIA (0-20 μM) for 4 h, and cell viability was measured by MTT assay. (C) H9c2 cells were pretreated with the indicated Tan IIA concentrations for 4 h followed by DOX (1 μM, 24 h) treatment, and cell viability was determined by MTT assay. (D) The cell morphological changes were detected via light microscopy (magnification, x200). (E) Intracellular ROS levels were measured with a fluorometric assay. (F) The content of intracellular GSH was measured with a GSH assay kit. Data are presented as mean ± standard error of the mean (n=3). *P<0.05, **P<0.01 and ***P<0.001 vs. the control; #P<0.05 and ##P<0.01 vs. DOX. Tan IIA, tanshinone IIA; DOX, doxorubicin; ROS, reactive oxygen species; GSH, glutathione; tBHQ, tertbutyl hydroquinone.

Nrf2 signaling is associated with the protective effect of Tan IIA on DOX-induced H9c2 cells injury. The mRNA expression of Nrf2 was significantly and dose-dependently increased following pretreatment with Tan IIA in DOX+Tan IIA group compared with the DOX alone group, as were HO-1, NQO1 and GCLC levels. Moreover, P-gp and MRP2 expression levels in the DOX + Tan IIA groups were decreased with 5 and 10 μM Tan IIA, but increased with 3 μM Tan IIA compared with DOX treatment alone, although they remained higher than those of the control (Fig. 5). Consistent with the mRNA data, Tan IIA pretreatment dose-dependently increased the protein expression of total Nrf2 compared with DOX alone (Fig. 6A and B). The nuclear and cytoplasmic Nrf2 accumulations were also investigated. As presented in Fig. 6C-E, Tan IIA (5 and 10 μM) pretreatment for 4 h prior to DOX treatment for 24 h significantly increased the nuclear level of Nrf2, whereas

no significant changes were observed at the cytoplasmic level with all Tan IIA dose or at the nuclear level with 3 μM Tan IIA.

Nrf2 knockdown inhibits the protective effect of Tan IIA on DOX-induced H9c2 cells injury. To further determine whether Tan IIA protected H9c2 cells against DOX-induced toxicity in a Nrf2-dependent manner, Nrf2-siRNA was transfected in H9c2 cells for 24 h to knockdown the Nrf2 expression. As presented in Fig. 7, the protein level of Nrf2 was reduced to 38.4±9.0% following Nrf2 siRNA transfection compared with that of the control. It was also observed that nuclear Nrf2 accumulated in the DOX + Tan IIA groups, and was significantly reduced in the Nrf2-siRNA + Tan IIA groups. Furthermore, the MTT assay presented in Fig. 8 revealed that DOX treatment significantly decreased the cell viability, while Tan IIA
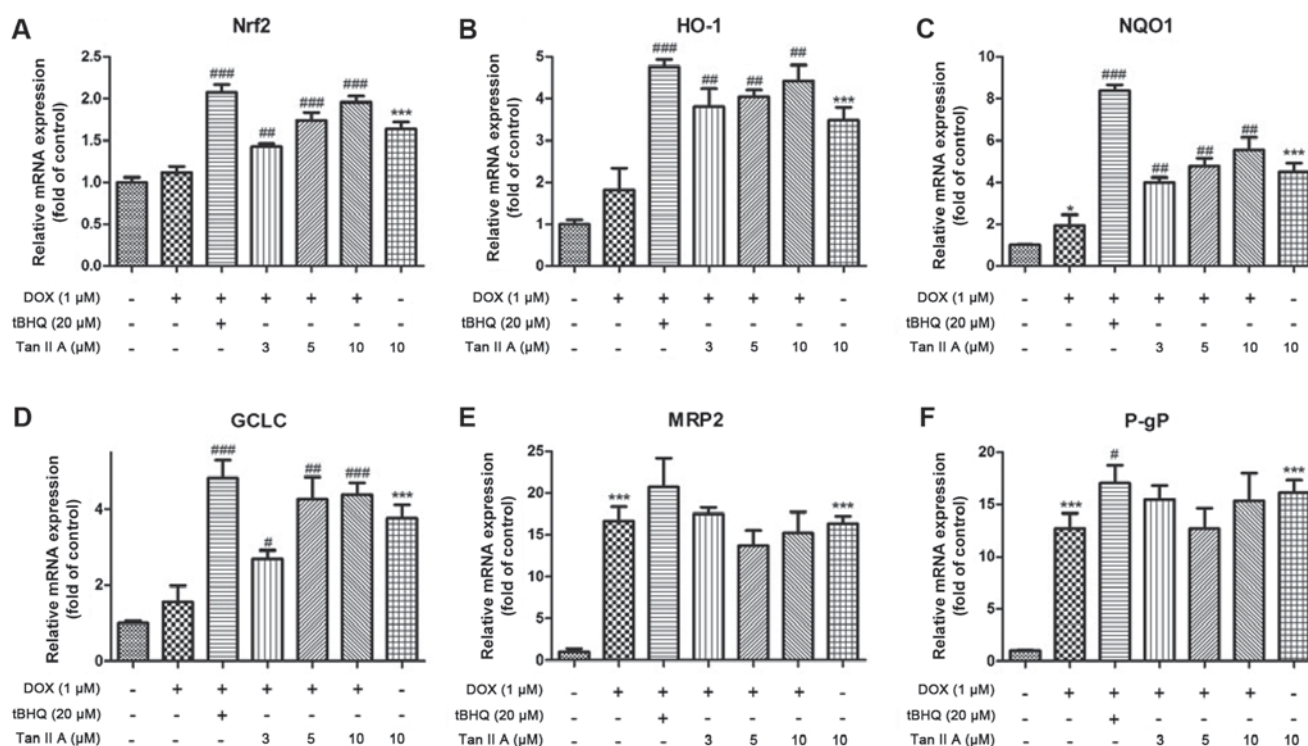
Figure 5. Effect of Tan IIA on relative mRNA expression of Nrf2 and its downstream genes in H9c2 cells. The mRNA expression of (A) Nrf2, and its downstream genes expression including (B) HO-1, (C) NQO1, (D) GCLC, (E) MRP2 and (F) P-gP were determined by reverse transcription-quantitative polymerase chain reaction. Data are presented as mean ± standard error of the mean (n=3). *P<0.05 and ***P<0.001 vs. the control; #P<0.05, ##P<0.01 and ###P<0.001 vs. DOX. Tan IIA, tanshinone IIA; Nrf2, nuclear factor (erythroid-derived) 2)-like 2; HO-1, heme oxygenase-1; NQO1, NAD(P)H dehydrogenase (quinone) 1; GCLC, glutamate-cysteine ligase catalytic subunit; MRP2, multidrug resistance-associated protein 2; P-gp, P-glycoprotein; DOX, doxorubicin; tBHQ, tertbutyl hydroquinone.

inhibited the effect of DOX on H9c2 cells, which is consistent with the results in Fig. 4C. Additionally, pre-transfection with Nrf2-siRNA to knockdown the Nrf2 expression reversed the effect of Tan IIA on the DOX-induced inhibition of cell viability. These results suggest that Nrf2 mediates the protective effect of Tan IIA on DOX-induced H9c2 cell injury.

Discussion

Nrf2 is a transcription factor that serves a key role in regulation of intracellular redox signaling (19). Under normal physiological conditions, Nrf2 is bound to Keap1 and located in the cytosol (20). The Keap1 protein contains several cysteine residues with sulfhydryl groups that can react with ROS and electrophiles (9). When cells are exposed to cellular stress, like ROS, the cysteine residues of Keap1 are modified by oxidative/electrophilic molecules, which results in breaking the bonds between Keap1 and Nrf2 (21). Once the bonds are broken, Nrf2 translocates to the cell nucleus and initiates transcription of antioxidant genes including SOD, NQO1, GCLC, HO-1, MRP2 and P-gP (22). Imbalance between free radicals and anti-oxidant defense is associated with cellular dysfunctions leading to the pathophysiology of various cardiovascular diseases (23). Therefore, Nrf2 may be considered as a key regulator in maintenance of normal cardiovascular function.

DOX is a widely used anti-cancer agent associated with irreversible cardiomyopathy (2). Although the precise cardiotoxicity mechanisms have not been clearly documented, it

is widely accepted that overproduction of ROS and oxidative stress have vital roles (5,24). In view of the potent antioxidant effect of Nrf2, several studies have investigated the role of Nrf2 in DOX-induced cardiotoxicity *in vivo* and *in vitro* (25,26). It has been reported that Nrf2 mediated the protective effect of sulforaphane, a-Linolenic acid and naringenin-7-O-glucoside on DOX-induced cardiotoxicity (7,10,11), which indicated that Nrf2 may be a guided drug target for DOX-induced cardiotoxicity.

Tan IIA, a major bioactive diterpene quinone of *Salva miltiorrhiza*, is used in the treatment of coronary heart disease, cerebrovascular disease, hepatitis and hepatocirrhosis due to its multiple pharmacological activities including anti-oxidant, anti-inflammatory and anti-neoplastic effects (12). The potential cardioprotective effects of Tan IIA on DOX-induced cardiotoxicity have been confirmed in animal models by decreasing the ST-interval and QRS interval, and improving the occurrence of myocardium fibrosis (14). On this basis, the present study further elucidated the inherent mechanism. Another previous study demonstrated that Tan IIA modulated Nrf2 expression in JB6 cells through epigenetic regulations (16). Others reported that Tan IIA inhibited atherosclerosis in endothelial cells via an Nrf2-related pathway (27). In the present study, it was not only discovered that Nrf2 nuclear accumulation was increased when treated with Tan IIA alone, but also that Tan IIA induced Nrf2 activity significantly in the Tan IIA + DOX-treated groups in mice and in H9c2 cells, and enhanced the expression of HO-1, NQO1 and GCLC. The essential role of Nrf2 in the protective effects of Tan IIA was further supported by the knock-down
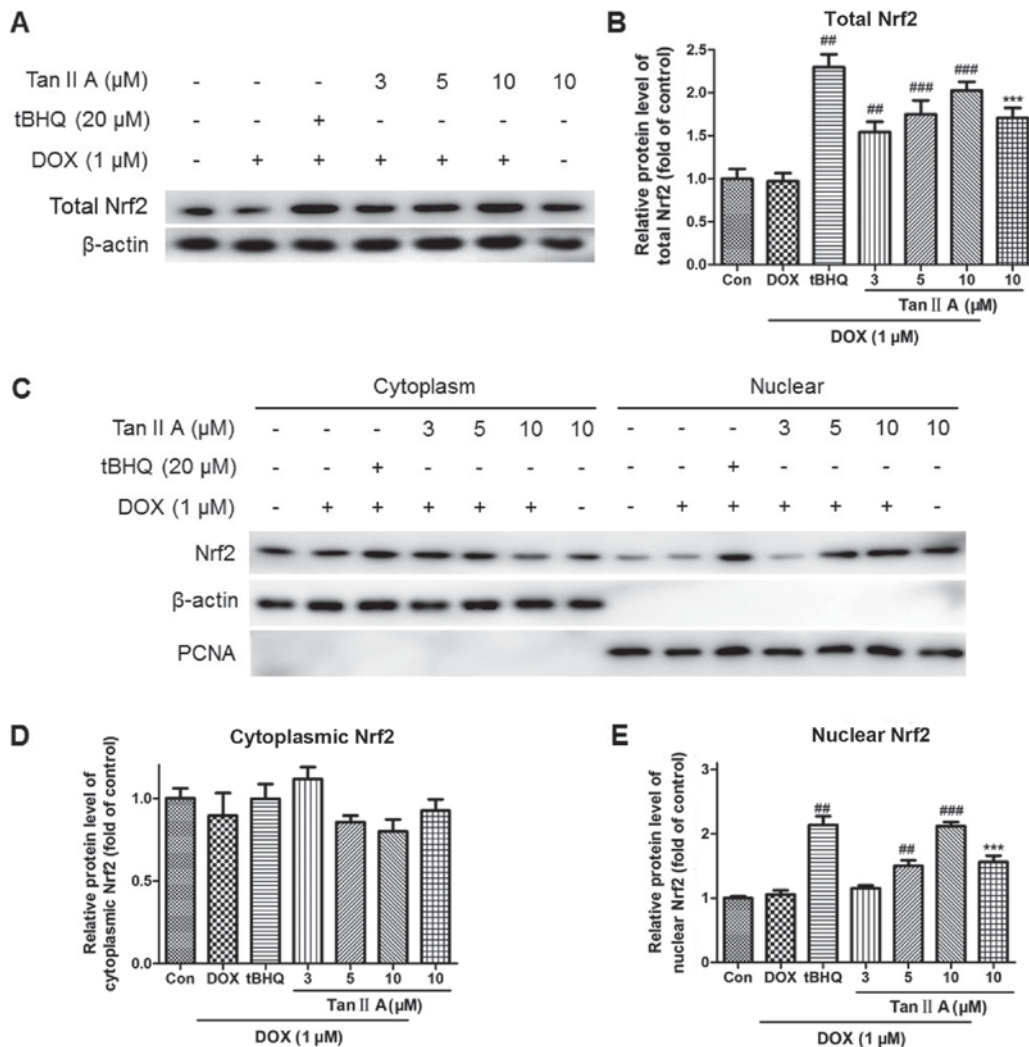
Figure 6. Effect of Tan IIA on Nrf2 protein expression in DOX-treated H9c2 cells. (A) Representative western blotting and (B) quantitative analysis of total Nrf2 protein expression. (C) Representative western blotting and (D and E) quantitative analysis of nuclear and cytoplasmic Nrf2 protein expression. Data are presented as mean ± standard error of the mean (n=3). ***P<0.001 vs. the control; $^{##}$P<0.01 and $^{###}$P<0.001 vs. DOX. Tan IIA, tanshinone IIA; Nrf2, nuclear factor (erythroid-derived 2)-like 2; DOX, doxorubicin; tBHQ, tertbutyl hydroquinone; PCNA, proliferating cell nuclear antigen.

experiments. Silencing the expression of Nrf2 by siRNA effectively suppressed the Tan IIA-induced activation of Nrf2 and at the same time reversed the increase in cell survival rate in the Tan IIA pretreatment groups. These data strongly suggest that the protective effect of Tan IIA on DOX-induced cardiotoxicity was at least partly mediated by the activation of the Nrf2 signaling pathway.

As Nrf2 induced downstream genes including antioxidants, phase II metabolism enzymes, and phase III drug transporters, HO-1, NQO1, GCLC, MRP2 and P-gp were focused on as they had been reported most in previous studies. HO-1 and NQO1 are known as important intracellular antioxidants to defend oxidative stress both inside and outside cells (28). GSH is vital in the detoxification of xenobiotics, and DOX treatment resulted in the depletion of GSH levels (29). GCLC is the catalytic subunit of GCL that catalyzes the rate-limiting step in the biosynthesis of GSH (30). Tan IIA activated these genes to decrease the oxidative burden by antioxidants and phase II conjugation reactions. However, although MRP2 and P-gp were also downstream targets of Nrf2, their expression exhibited no

significant changes compared with Tan IIA pretreatment groups with DOX alone. MRP2 and P-gp are phase III drug transporters which can remove xenobiotics and metabolites that accumulate in the tissues and lead to toxicity. However, such transporters are more likely to be studied in metabolism organs like the liver and the kidney (31). Few studies on transporters in the heart have been published, to the best of our knowledge, suggesting that transporters are not the main target of drugs or toxins in the heart. Conversely, Tan IIA has mostly been demonstrated to have anti-oxidant and anti-inflammation properties, and the ability of Tan IIA to modulate drug transporters, particularly MRP2 and P-gp, may be quite weak (12). In addition, there may be other signal pathways that can modulate MRP2 and P-gp other than Nrf2.

Notably, it was observed that DOX-treatment induced oxidative stress but did not activate Nrf2 in the present study. In addition to Nrf2, many other factors are associated with DOX-treatment induce oxidative stress, including NADPH and NQO1 (32,33). This may be the cause of the present result. To the best of our knowledge, previous studies have investigated the effect of DOX-treatment on Nrf2 nuclear accumulation,
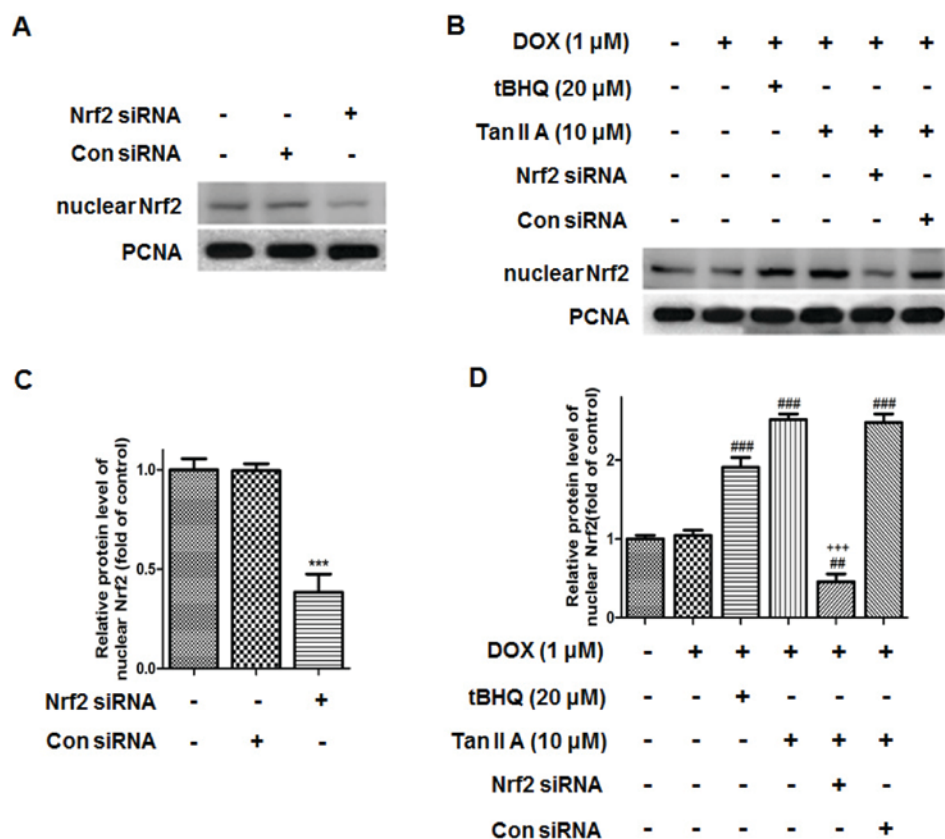
Figure 7. Effect of Nrf2 siRNA on the protein expression of nuclear Nrf2 in H9c2 cells. The protein expression of nuclear Nrf2 upon (A) Nrf2 siRNA treatment, and (B) subsequent treatment with DOX, tBHQ and Tan IIA was determined by western blotting, (C and D) and quantitatively analysed. Data are presented as mean ± standard error of the mean (n=3). ***P<0.001 vs. NC, ##P<0.01 and ###P<0.001 vs. DOX; +++P<0.001 vs. DOX + Tan IIA (10 μM). Nrf2, nuclear factor (erythroid-derived 2)-like 2; siRNA, small interfering RNA; DOX, doxorubicin; tBHQ, tertbutyl hydroquinone; Tan IIA, tanshinone IIA; NC, siRNA negative control; PCNA, proliferating cell nuclear antigen.
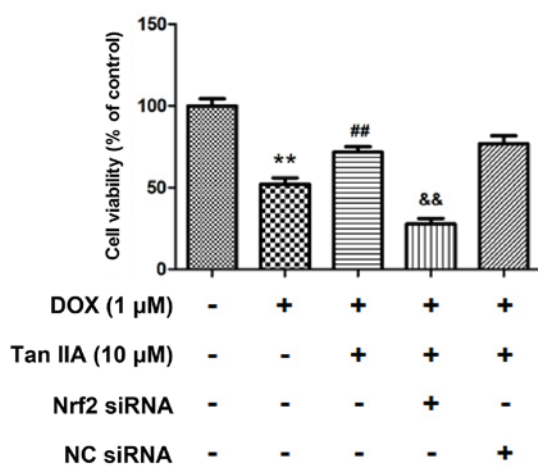

Figure 8. Effect of Tan IIA pretreatment on H9c2 cells viability following Nrf2-siRNA transfection. The cell viability was measured by MTT. Data are presented as mean ± standard error of the mean (n=3). **P<0.01 vs. control; ##P<0.01 vs. DOX; &&P<0.01 vs. DOX+Tan IIA. DOX, doxorubicin; Tan IIA, tanshinone IIA; Nrf2, nuclear factor (erythroid-derived 2)-like 2; siRNA, small interfering RNA; NC, siRNA negative control.

however, yet received inconsistent results. Li *et al* (7) and Han *et al* (10) demonstrated that DOX-treatment can inhibit the Nrf2 nuclear transport, whereas Yu *et al* (11) received

the opposite result. These inconsistent results may be due to different treatment times and concentrations.

Although several natural or synthetic compounds may be used to prevent DOX-induced cardiotoxicity (34-36), one of the major advantages of Tan IIA is that it has already been used in clinic settings to treat coronary heart disease and angina pectoris as Tan IIA sodium sulfonate injection with acceptable bioavailability (37). The dose of Tan IIA used in humans was 1.5 mg/kg, whereas 30 mg/kg in mice (15), as used in the present study, can be converted to 4.95 mg/kg in human. This suggests that the dose of Tan IIA for treating DOX-induced cardiotoxicity in clinical settings may need to be raised to >3 times as much as the dose that patients are currently treated with. Furthermore, Tan IIA was previously demonstrated to be able to suppress the proliferation of cancer cells and exhibit anticancer activity (38-40), which may improve anti-cancer potency when used together with DOX.

A previous study demonstrated the protective effect of Tan IIA against DOX-induced cardiotoxicity (14), but there were several limitations. It has previously been suggested that H9c2 cells were undifferentiated myoblasts, which may not be considered as cardiomyocytes (41). Furthermore, the study by Jiang *et al* (14) demonstrated that cell viability was not sufficient to indicate the protective effects of Tan IIA against DOX-induced cardiotoxicity. More functional assays may be required in future studies in primary cardiomyocytes to verify

the protective effects of Tan IIA, such as alteration of cell cycle and apoptosis-related protein expressions.

In conclusion, the present study suggests that the Nrf2-dependent antioxidant response mediates the protective effect of Tan IIA on DOX-induced cardiotoxicity, indicating that Tan IIA may be a promising therapeutic adjuvant that may prevent the heart from serious side effects of DOX. Furthermore, these findings emphasize the vital role of Nrf2 signaling as promising targets to identify more potent pharmacological agents against DOX-induced cardiotoxicity.

Acknowledgements

Availability of data and materials

The datasets used or analyzed during the present study are available from the corresponding author on reasonable request.

Authors' contributions

MY, WL and BZ designed the experiments. ZG, LC, PF, ZL, ZW, SC, ZH and SW performed the experiments. ZG and WL analyzed the data. WL and BZ wrote the manuscript.

Ethics approval and consent to participate

All animal use procedures were conducted according to the Regulations of Experimental Animal Administration issued by the State Committee of Science and Technology of the People's Republic of China, with the approval of the Ethics Committee of The Experimental Animal Center of the Second Xiangya Hospital (Changsha, China).

Patient consent for publication

Not applicable.

Competing interests

The authors declare that they have no competing interests.

References

1. Gorini S, De Angelis A, Berrino L, Malara N, Rosano G and Ferraro E: Chemotherapeutic drugs and mitochondrial dysfunction: Focus on doxorubicin, trastuzumab, and sunitinib. Oxid Med Cell Longev 2018: 7582730, 2018.
2. Vejpongsa P and Yeh ET: Prevention of anthracycline-induced cardiotoxicity: Challenges and opportunities. J Am Coll Cardiol 64: 938-945, 2014.
3. van Dalen EC, van der Pal HJ, Caron HN and Kremer LC: Different dosage schedules for reducing cardiotoxicity in cancer patients receiving anthracycline chemotherapy. Cochrane Database Syst Rev: CD005008, 2006.
4. Pugazhendhi A, Edison TNJI, Velmurugan BK, Jacob JA and Karuppusamy I: Toxicity of doxorubicin (Dox) to different experimental organ systems. Life Sci 200: 26-30, 2018.
5. Carvalho FS, Burgeiro A, Garcia R, Moreno AJ, Carvalho RA and Oliveira PJ: Doxorubicin-induced cardiotoxicity: From bioenergetic failure and cell death to cardiomyopathy. Med Res Rev 34: 106-135, 2014.
6. Chen CT, Wang ZH, Hsu CC, Lin HH and Chen JH: In vivo protective effects of diosgenin against doxorubicin-induced cardiotoxicity. Nutrients 7: 4938-4954, 2015.
7. Li B, Kim DS, Yadav RK, Kim HR and Chae HJ: Sulforaphane prevents doxorubicin-induced oxidative stress and cell death in rat H9c2 cells. Int J Mol Med 36: 53-64, 2015.
8. Howden R: Nrf2 and cardiovascular defense. Oxid Med Cell Longev 2013: 104308, 2013.
9. Ma Q and He X: Molecular basis of electrophilic and oxidative defense: Promises and perils of Nrf2. Pharmacol Rev 64: 1055-1081, 2012.
10. Han X, Pan J, Ren D, Cheng Y, Fan P and Lou H: Naringenin-7-O-glucoside protects against doxorubicin-induced toxicity in H9c2 cardiomyocytes by induction of endogenous antioxidant enzymes. Food Chem Toxicol 46: 3140-3146, 2008.
11. Yu X, Cui L, Zhang Z, Zhao Q and Li S: α-Linolenic acid attenuates doxorubicin-induced cardiotoxicity in rats through suppression of oxidative stress and apoptosis. Acta Biochim Biophys Sin (Shanghai) 45: 817-826, 2013.
12. Xu S and Liu P: Tanshinone II-A: New perspectives for old remedies. Expert Opin Ther Pat 23: 149-153, 2013.
13. Gao S, Liu Z, Li H, Little PJ, Liu P and Xu S: Cardiovascular actions and therapeutic potential of tanshinone IIA. Atherosclerosis 220: 3-10, 2012.
14. Jiang B, Zhang L, Wang Y, Li M, Wu W, Guan S, Liu X, Yang M, Wang J and Guo DA: Tanshinone IIA sodium sulfonate protects against cardiotoxicity induced by doxorubicin in vitro and in vivo. Food Chem Toxicol 47: 1538-1544, 2009.
15. Wang W, Guan C, Sun X, Zhao Z, Li J, Fu X, Qiu Y, Huang M, Jin J and Huang Z: Tanshinone IIA protects against acetaminophen-induced hepatotoxicity via activating the Nrf2 pathway. Phytomedicine 23: 589-596, 2016.
16. Wang L, Zhang C, Guo Y, Su ZY, Yang Y, Shu L and Kong AN: Blocking of JB6 cell transformation by tanshinone IIA: Epigenetic reactivation of Nrf2 antioxidative stress pathway. AAPS J 16: 1214-1225, 2014.
17. Livak KJ and Schmittgen TD: Analysis of relative gene expression data using real-time quantitative PCR and the 2(-Delta Delta C(T)) method. Methods 25: 402-408, 2001.
18. Alam MF, Khan G, Safhi MM, Alshahrani S, Siddiqui R, Sivagurunathan Moni S and Anwer T: Thymoquinone ameliorates doxorubicin-induced cardiotoxicity in swiss albino mice by modulating oxidative damage and cellular inflammation. Cardiol Res Pract 2018: 1483041, 2018.
19. Sies H, Berndt C and Jones DP: Oxidative stress. Annu Rev Biochem 86: 715-748, 2017.
20. Bellezza I, Giambanco I, Minelli A and Donato R: Nrf2-Keap1 signaling in oxidative and reductive stress. Biochim Biophys Acta 1865: 721-733, 2018.
21. Silva-Islas CA and Maldonado PD: Canonical and non-canonical mechanisms of Nrf2 activation. Pharmacol Res 134: 92-99, 2018.
22. Jiang S, Yang Y, Li T, Ma Z, Hu W, Deng C, Fan C, Lv J, Sun Y and Yi W: An overview of the mechanisms and novel roles of Nrf2 in cardiovascular diseases. Expert Opin Ther Targets 20: 1413-1424, 2016.
23. Ramprasath T, Vasudevan V, Sasikumar S, Puhari SS, Saso L and Selvam GS: Regression of oxidative stress by targeting eNOS and Nrf2/ARE signaling: A guided drug target for cardiovascular diseases. Curr Top Med Chem 15: 857-871, 2015.
24. Tacar O, Sriamornsak P and Dass CR: Doxorubicin: An update on anticancer molecular action, toxicity and novel drug delivery systems. J Pharm Pharmacol 65: 157-170, 2013.
25. Li S, Wang W, Niu T, Wang H, Li B, Shao L, Lai Y, Li H, Janicki JS, Wang XL, et al: Nrf2 deficiency exaggerates doxorubicin-induced cardiotoxicity and cardiac dysfunction. Oxid Med Cell Longev 2014: 748524, 2014.
26. Wang LF, Su SW, Wang L, Zhang GQ, Zhang R, Niu YJ, Guo YS, Li CY, Jiang WB, Liu Y and Guo HC: Tert-butylhydroquinone ameliorates doxorubicin-induced cardiotoxicity by activating Nrf2 and inducing the expression of its target genes. Am J Transl Res 7: 1724-1735, 2015.

27. Liu Z, Wang J, Huang E, Gao S, Li H, Lu J, Tian K, Little PJ, Shen X, Xu S and Liu P: Tanshinone IIA suppresses cholesterol accumulation in human macrophages: Role of heme oxygenase-1. J Lipid Res 55: 201-213, 2014.

28. Sarkar S, Mukherjee S, Chattopadhyay A and Bhattacharya S: Low dose of arsenic trioxide triggers oxidative stress in zebrafish brain: Expression of antioxidant genes. Ecotoxicol Environ Saf 107: 1-8, 2014.

29. Cheraghi M, Namdari M, Daraee H and Negahdari B: Cardioprotective effect of magnetic hydrogel nanocomposite loaded N,α-L-rhamnopyranosyl vincosamide isolated from Moringa oleifera leaves against doxorubicin-induced cardiac toxicity in rats: In vitro and in vivo studies. J Microencapsul 34: 335-341, 2017.

30. Zhu H, Long MH, Wu J, Wang MM, Li XY, Shen H, Xu JD, Zhou L, Fang ZJ, Luo Y and Li SL: Ginseng alleviates cyclophosphamide-induced hepatotoxicity via reversing disordered homeostasis of glutathione and bile acid. Sci Rep 5: 17536, 2015.

31. Kawase A, Norikane S, Okada A, Adachi M, Kato Y and Iwaki M: Distinct alterations in ATP-binding cassette transporter expression in liver, kidney, small intestine, and brain in adjuvant-induced arthritic rats. J Pharm Sci 103: 2556-2564, 2014.

32. Park J, Park E, Ahn BH, Kim HJ, Park JH, Koo SY, Kwak HS, Park HS, Kim DW, Song M, *et al*: NecroX-7 prevents oxidative stress-induced cardiomyopathy by inhibition of NADPH oxidase activity in rats. Toxicol Appl Pharmacol 263: 1-6, 2012.

33. Hajra S, Patra AR, Basu A and Bhattacharya S: Prevention of doxorubicin (DOX)-induced genotoxicity and cardiotoxicity: Effect of plant derived small molecule indole-3-carbinol (I3C) on oxidative stress and inflammation. Biomed Pharmacother 101: 228-243, 2018.

34. Al-Harthi SE, Alarabi OM, Ramadan WS, Alaama MN, Al-Kreathy HM, Damanhouri ZA, Khan LM and Osman AM: Amelioration of doxorubicininduced cardiotoxicity by resveratrol. Mol Med Rep 10: 1455-1460, 2014.

35. Thandavarayan RA, Giridharan VV, Arumugam S, Suzuki K, Ko KM, Krishnamurthy P, Watanabe K and Konishi T: Schisandrin B prevents doxorubicin induced cardiac dysfunction by modulation of DNA damage, oxidative stress and inflammation through inhibition of MAPK/p53 signaling. PLoS One 10: e0119214, 2015.

36. Chen RC, Xu XD, Zhi Liu X, Sun GB, Zhu YD, Dong X, Wang J, Zhang HJ, Zhang Q and Sun XB: Total flavonoids from clinopodium chinense (Benth.) O. Ktze protect against doxorubicin-induced cardiotoxicity in vitro and in vivo. Evid Based Complement Alternat Med 2015: 472565, 2015.

37. Chen Y, Tu JH, He YJ, Zhang W, Wang G, Tan ZR, Zhou G, Fan L and Zhou HH: Effect of sodium tanshinone II A sulfonate on the activity of CYP1A2 in healthy volunteers. Xenobiotica 39: 508-513, 2009.

38. Munagala R, Aqil F, Jeyabalan J and Gupta RC: Tanshinone IIA inhibits viral oncogene expression leading to apoptosis and inhibition of cervical cancer. Cancer Lett 356: 536-546, 2015.

39. Su CC: Tanshinone IIA potentiates the efficacy of 5-FU in Colo205 colon cancer cells in vivo through downregulation of P-gp and LC3-II. Exp Ther Med 3: 555-559, 2012.

40. Lin C, Wang L, Wang H, Yang L, Guo H and Wang X: Tanshinone IIA inhibits breast cancer stem cells growth in vitro and in vivo through attenuation of IL-6/STAT3/NF-kB signaling pathways. J Cell Biochem 114: 2061-2070, 2013.

41. Branco AF, Sampaio SF, Moreira AC, Holy J, Wallace KB, Baldeiras I, Oliveira PJ and Sardão VA: Differentiation-dependent doxorubicin toxicity on H9c2 cardiomyoblasts. Cardiovasc Toxicol 12: 326-340, 2012.